Preprints of the 19th World Congress
The International Federation of Automatic Control
Cape Town, South Africa. August 24-29, 2014

Two upper bounds on the $\mathcal{H}_\infty$-norm of LTI dynamical systems

Pierre Vuillemin * **Charles Poussot-Vassal** ** **Daniel Alazard** *

* *Université de Toulouse and Onera - The French Aerospace Lab, F-31055 Toulouse, France (email : pierre.vuillemin@onera.fr)*
** *Onera - The French Aerospace Lab, F-31055 Toulouse, France*

Abstract: The poles/residues expression of the frequency-limited $\mathcal{H}_2$-norm is used to derive two upper bounds on the $\mathcal{H}_\infty$-norm of a MIMO LTI dynamical system. These bounds can be efficiently computed when the eigenvalues and eigenvectors of the model are available. This specificity make them particularly well suited to watch the $\mathcal{H}_\infty$-norm of the approximation error in the context of the frequency-limited $\mathcal{H}_2$ model approximation method suggested recently by the authors.The efficiency of these bounds, as well as their integration in the model approximation algorithm are illustrated through several numerical examples.

Keywords: $\mathcal{H}_\infty$-norm, LTI dynamical systems, model approximation

1. INTRODUCTION

The optimal $\mathcal{H}_2$ model approximation problem has recently known several advances especially through the methods proposed in Gugercin et al. (2008) or Van Dooren et al. (2008). They perform rational or tangential interpolation in particular complex points to achieve optimal $\mathcal{H}_2$ model approximation and are numerically efficient in practice, even on (very) large-scale models. Yet, due to sensors and actuators limited bandwidth, it may be more relevant to build a reduced order model that matches well the large-scale one in a bounded frequency range. This can be done by considering the frequency-limited $\mathcal{H}_2$-norm, denoted here $\mathcal{H}_{2,\Omega}$-norm, as criterion in the approximation process.

To the authors' knowledge, the $\mathcal{H}_{2,\Omega}$-norm (see Definition 1) has firstly been suggested in Anderson et al. (1991) to perform frequency analysis of nominally unstable systems. More recently it has been used in robust analysis (Masi et al. (2010)) and comfort analysis (Poussot-Vassal et al. (2013)). The norm is also closely related to the frequency-limited gramians implied in the frequency-limited balanced truncation (Gawronski and Juang (1990)) since it can be computed with one of them, similarly to the $\mathcal{H}_2$-norm.

Definition 1. ($\mathcal{H}_{2,\Omega}$-norm). The $\mathcal{H}_{2,\Omega}$-norm of a LTI dynamical system with transfer function H, is defined as the restriction of the $\mathcal{H}_2$-norm over $\Omega = [0, \omega]$, $\omega \in \mathbb{R}_+^*$, *i.e.*

$$\|H\|_{\mathcal{H}_{2,\Omega}} = \sqrt{\frac{1}{2\pi}\int_{-\omega}^{\omega} \mathbf{tr}\left(H(j\nu)H(-j\nu)^T\right) d\nu}. \quad (1)$$

Based on this norm, the frequency-limited model approximation problem is stated in Problem 1.

Problem 1. Let us consider a n-th order LTI dynamical system realization $\mathbf{H}$ with n_u inputs and n_y outputs, described by its transfer function H as

$$H(s) = C(sI_n - A)^{-1}B + D \in \mathbb{C}^{n_y \times n_u}, \quad (2)$$

where $A \in \mathbb{R}^{n\times n}$, $B \in \mathbb{R}^{n\times n_u}$, $C \in \mathbb{R}^{n_y\times n}$ and $D \in \mathbb{R}^{n_y\times n_u}$. The goal is to find a reduced order model $\hat{\mathbf{H}}$ with transfer function $\hat{H}$,

$$\hat{H}(s) = \hat{C}(sI_r - \hat{A})^{-1}\hat{B} + \hat{D} \in \mathbb{C}^{n_y\times n_u}, \quad (3)$$

where $\hat{A} \in \mathbb{R}^{r\times r}$, $\hat{B} \in \mathbb{R}^{r\times n_u}$, $\hat{C} \in \mathbb{R}^{n_y\times r}$ and $\hat{D} \in \mathbb{R}^{n_y\times n_u}$ with $r \ll n$ such that $\hat{H}(s)$ minimizes the frequency-limited $\mathcal{H}_2$-norm of the error system, *i.e.*

$$\|H - \hat{H}\|_{\mathcal{H}_{2,\Omega}}^2 = \min_{G\ stable} \|H - G\|_{\mathcal{H}_{2,\Omega}}^2 = \min_{G\ stable} \mathcal{J}_{\mathcal{H}_{2,\Omega}}. \quad (4)$$

The frequency-limited $\mathcal{H}_2$-norm can be computed either with the frequency-limited gramians or with the poles and residues of the model's transfer function (Vuillemin et al. (2012)). Both formulations have been used to address Problem 1. Indeed, optimization schemes have been introduced in Petersson (2013) and Vuillemin et al. (2014), based on the gramian and poles/residues formulations, respectively, to perform optimal $\mathcal{H}_{2,\Omega}$ model approximation. Those approaches ensure a decrease of the $\mathcal{H}_{2,\Omega}$ error, but there is no indication on the $\mathcal{H}_\infty$-norm of the error unlike the balanced truncation, which offers an upper bound. In this article, we propose two new upper bounds of the $\mathcal{H}_\infty$-norm of LTI dynamical systems. Since these bounds are based on the poles/residues formulation of the frequency-limited $\mathcal{H}_2$-norm, they naturally fit within the optimization scheme for model approximation purpose presented in Vuillemin et al. (2014). Indeed, computing the $\mathcal{H}_\infty$ bounds of the approximation error results only in very few extra numerical costs.

The paper is divided as follows : in Section 3, the two upper bounds on the $\mathcal{H}_\infty$-norm of a LTI dynamical system are proposed. Section 2 then presents the integration of those bounds in a recently proposed optimization algorithm for frequency-limited model approximation. Then, in Section 4, the behaviour of the two bounds is illustrated though several examples. Finally Section 5 concludes the paper.

2. TWO UPPER BOUNDS ON THE $\mathcal{H}_\infty$-NORM OF LTI MIMO SYSTEMS

In this section, two bounds on the $\mathcal{H}_\infty$-norm are introduced. The first bound is obtained through an optimization process, whereas the second bound is more conservative but analytically obtained. Both bounds are grounded on the poles/residues expression of the frequency-limited $\mathcal{H}_2$-norm recalled thereafter.

2.1 Poles/residues formulation of the $\mathcal{H}_{2,\Omega}$-norm

If the matrix A arising in (2) is diagonalizable, then $H(s)$ can be written as

$$H(s) = \sum_{i=1}^{n} \frac{\phi_i}{s-\lambda_i} + D, \tag{5}$$

where λ_i, ϕ_i $(i = 1,\ldots,n)$ are the poles and associated residues of the transfer function. The poles/residues expression of $\|H\|_{\mathcal{H}_{2,\Omega}}$ is based on this partial fraction expansion and is recalled in Theorem 1.

Theorem 1. (Vuillemin et al. (2012)). Let us consider a transfer function as in (5), a frequency band $\Omega = [0,\omega]$, $\omega > 0$, and $\mathbf{a}_{\omega,i} = \frac{2}{\pi}\mathbf{atan}\left(\frac{\omega}{\lambda_i}\right)$ where $\mathbf{atan}(z)$ is the principal value of the arctangent of $z \in \mathbb{C}\setminus\{j,-j\}$, then the $\mathcal{H}_{2,\Omega}$-norm of H, can be expressed as,

$$\|H\|^2_{\mathcal{H}_{2,\Omega}} = \mathbf{tr}\left(\sum_{i=1}^{n} -\phi_i H(-\lambda_i)^T \mathbf{a}_{\omega,i} + \frac{\omega}{\pi} DD^T\right). \tag{6}$$

Proof : See Vuillemin et al. (2012). □

Remark 1. (Strictly proper case). When $D = 0$, the expression (6) simplifies in

$$\|H\|^2_{\mathcal{H}_{2,\Omega}} = \mathbf{tr}\left(\sum_{i=1}^{n} -\phi_i H(-\lambda_i)^T \mathbf{a}_{\omega,i}\right), \tag{7}$$

which is similar to the poles/residues expression of the $\mathcal{H}_2$-norm given in Antoulas (2005),

$$\|H\|^2_{\mathcal{H}_2} = \mathbf{tr}\left(\sum_{i=1}^{n} \phi_i H(-\lambda_i)^T\right), \tag{8}$$

excepted from the weightings coefficients $\mathbf{a}_{\omega,i}$. Moreover, if H is stable, as ω tends towards infinity, $\mathbf{a}_{\omega,i}$ tends towards -1 (see Haber (2011)), hence

$$\lim_{\omega\to\infty} \|H\|^2_{\mathcal{H}_{2,\Omega}} = \|H\|^2_{\mathcal{H}_2}. \tag{9}$$

Remark 2. (Multiples frequency intervals). The frequency-limited $\mathcal{H}_2$-norm can also be computed on more complex intervals. Indeed, considering $\Omega = \Omega_1 \bigcap \Omega_2$ where $\Omega_1 = [0,\omega_1]$ and $\Omega_2 = [0,\omega_2]$ with $\omega_1 < \omega_2$ then

$$\|H\|^2_{\mathcal{H}_{2,\Omega}} = \|H\|^2_{\mathcal{H}_{2,\Omega_2}} - \|H\|^2_{\mathcal{H}_{2,\Omega_1}}. \tag{10}$$

2.2 Link between the $\mathcal{H}_\infty$ and $\mathcal{H}_{2,\Omega}$ norms

The link between the $\mathcal{H}_\infty$-norm, recalled in Definition 2, and the $\mathcal{H}_{2,\Omega}$-norm, is presented in Theorem 2. It is grounded on the Frobenius norm which is recalled in Definition 3. Since the extension is straightforward, only the strictly proper case is addressed in the sequel.

Definition 2. ($\mathcal{H}_\infty$-norm). The $\mathcal{H}_\infty$-norm of a LTI dynamical system H, is defined as

$$\|H\|_{\mathcal{H}_\infty} := \max_{\omega\in\mathbb{R}} \sigma_{max}\left(H(j\omega)\right), \tag{11}$$

where $\sigma_{max}\left(H(j\omega)\right)$ is the largest singular value of $H(j\omega)$.

Definition 3. (Frobenius norm). The Frobenius norm of a matrix $M \in \mathbb{C}^{m\times n}$ is given by

$$\|M\|_F := \sqrt{\mathbf{tr}\left(MM^H\right)} = \sqrt{\sum_{i=1}^{min(m,n)} \sigma_i^2}, \tag{12}$$

where the σ_i, $i = 1,\ldots,min\,(m,n)$ are the singular values of M.

Theorem 2. ($\mathcal{H}_\infty$ upper bound). Let us consider a stable LTI dynamical system H, its $\mathcal{H}_\infty$-norm is upper bounded as

$$\|H\|_{\mathcal{H}_\infty} \leq \max_{\omega\in\mathbb{R}} \sqrt{\pi \frac{d\|H\|^2_{\mathcal{H}_{2,\Omega}}}{d\omega}}. \tag{13}$$

Proof : Considering the definition of the $\mathcal{H}_\infty$-norm, it comes that

$$\|H\|_{\mathcal{H}_\infty} \leq \max_{\omega\in\mathbb{R}} \|H(j\omega)\|_F. \tag{14}$$

The $\mathcal{H}_{2,\Omega}$-norm can be written as the integral of the transfer function's Frobenius norm over $[-\omega,\omega]$,

$$\|H\|^2_{\mathcal{H}_{2,\Omega}} = \frac{1}{2\pi}\int_{-\omega}^{\omega} \|H(j\nu)\|^2_F \, d\nu. \tag{15}$$

Thus by differentiating this expression with respect to ω, it comes that

$$\|H(j\omega)\|^2_F = \pi \frac{d\|H\|^2_{\mathcal{H}_{2,\Omega}}}{d\omega}, \tag{16}$$

which concludes the proof. □

Remark 3. (SISO case). For SISO systems, the bound (13) becomes an equality.

The bound presented in Theorem 2 (equation (13)) can be conveniently expressed based on the spectral expression of the frequency-limited $\mathcal{H}_2$-norm. Indeed, by differentiating (7) with respect to ω, it comes that

$$\frac{d\|H\|^2_{\mathcal{H}_{2,\Omega}}}{d\omega} = -\frac{2}{\pi}\sum_{i=1}^{n} \mathbf{tr}\left(\phi_i H(-\lambda_i)^T\right)\frac{\lambda_i}{\lambda_i^2+\omega^2} = \sum_{i=1}^{n} f_i(\omega). \tag{17}$$

Each function f_i is a scalar complex valued function but the sum is real (each function comes with its complex conjugate in the sum). Therefore, only the real parts of the functions f_i need to be considered. By denoting

$$\begin{aligned} x_i + jy_i &= \lambda_i \quad \text{and} \\ a_i + jb_i &= -\frac{2}{\pi}\mathbf{tr}\left(\phi_i H(-\lambda_i)^T\right)\lambda_i, \end{aligned} \tag{18}$$

it comes that, for $i = 1,\ldots,n$,

$$g_i(\omega) = \mathbf{Re}\left(f_i(\omega)\right) = \frac{a_i(x_i^2 - y_i^2 + \omega^2) + 2b_i y_i x_i}{(x_i^2 - y_i^2 + \omega^2)^2 + 4x_i^2 y_i^2}. \tag{19}$$

Grounded on this formulation, two upper bounds are proposed in Theorem 3.

Theorem 3. $\mathcal{H}_\infty$-norm upper bounds Given a MIMO LTI dynamical system $\mathbf{H}$ of order n with a diagonalizable realization matrix A, its $\mathcal{H}_\infty$-norm is bounded by Γ and $\bar{\Gamma}$ as follows,

$$\|H\|_{\mathcal{H}_\infty} \leq \underbrace{\sqrt{\max_{\omega\in\mathbb{R}} \pi \sum_{i=1}^{n} g_i(\omega)}}_{\Gamma} \leq \underbrace{\sqrt{\pi \sum_{i=1}^{n} \max_{\omega\in\mathbb{R}} g_i(\omega)}}_{\bar{\Gamma}} \quad (20)$$

where the functions g_i are defined in (19).

2.3 Practical computation of the bounds

The two upper bounds proposed in Theorem 3 are obtained as follows :

- Computing $\bar{\Gamma}$ consists in finding the maximums of n simple rational functions. This can be achieved analytically.
- Computing Γ consists in finding the maximum of a sum of rational functions. This can be achieved by a standard optimization algorithm.

Computation of $\bar{\Gamma}$: in order to compute $\bar{\Gamma}$, the maximum of each function g_i has to be found, this is done by expressing the stationary points of the functions. The derivative of g_i $(i = 1, \ldots, n)$ with respect to ω is given by,

$$g_i'(\omega) = \frac{2\omega N_i(\omega)}{((x_i^2 - y_i^2 + \omega^2)^2 + 4x_i^2 y_i^2)^2}, \quad (21)$$

where,

$$N_i(\omega) = [(x_i^2 - y_i^2 + \omega^2)(-a_i(x_i^2 - y_i^2 + \omega^2) - 4b_i y_i x_i) \ldots + 4a_i x_i^2 y_i^2]. \quad (22)$$

The stationary points are then given by the zeros of the numerator, *i.e.* 0 and the roots $p_{i,k}$, $k = 1, \ldots, 4$ of the polynomial N_i which are

$$p_{i,k} = \pm\sqrt{\pm 2\frac{\sqrt{x_i^2 y_i^2 (a_i^2 + b_i^2)}}{a_i} - \frac{2b_i x_i y_i}{a_i} - x_i^2 + y_i^2}. \quad (23)$$

The functions g_i have no real pole and tends towards 0 as ω tends towards infinity, hence they are bounded on $\mathbb{R}$. In particular, they are bounded either by 0 when they are strictly negative, or by their value at one of the stationary points. This property is used in Algorithm 1 to compute the bound $\bar{\Gamma}$.

Algorithm 1 Computation of $\bar{\Gamma}$

Require: The model's state space realization (A, B, C).
1: Compute the eigenvalue decomposition of A, *i.e.* $AV = V\Delta$, where $\Delta = \mathbf{diag}(\lambda_1, \ldots, \lambda_n)$.
2: Compute a_i, b_i, x_i and y_i $i = 1, \ldots, n$ from (18).
3: **for** $i = 1, \ldots, n$ **do**
4: Compute $p_{i,k}$, $k = 1, \ldots, 4$, with (23).
5: Evaluate $g_i(0)$ and $g_i(r_{i,j})$ where $r_{i,j}$, $j = 1, \ldots, n_r$ are the n_r real values of the roots $p_{i,k}$, $k = 1, \ldots, 4$.
6: Set $\bar{g}_i = \max\{0, g_i(0), g_i(r_{i,j})\}$.
7: **end for**
8: Set $\bar{\Gamma} = \sqrt{\pi \sum_{i=1}^{n} \bar{g}_i}$.

Note that to determine a_i and b_i, $i = 1, \ldots, n$ (step 2), the residues should not explicitly be constructed. Indeed, by denoting $\odot$ the Hadamard product between two matrices,

$$[\, a_1 + jb_1 \ \ldots \ a_n + jb_n \,]^T = \left(\left(c^T c\right) \odot \left(bb^T\right) \odot L\right) \mathbb{1}, \quad (24)$$

where $c = CV \in \mathbb{C}^{n_y \times n}$, $b = V^{-1}B \in \mathbb{C}^{n \times n_u}$, $\mathbb{1} \in \mathbb{R}^{n \times 1}$ is a column vector full of 1 and $L \in \mathbb{C}^{n \times n}$ is the matrix which i, j-th element is given by $[L]_{i,j} = \frac{2}{\pi}\frac{\lambda_i}{\lambda_i + \lambda_j}$.

Computation of Γ : Finding Γ requires to find the global maximum of a non-convex function composed by a sum of rational functions. Specific approaches address this complex issue (Bugarin et al. (2011)), but since a good initial point is available, a more straightforward approach has been considered here. Indeed, only a local optimization process is used together with a good initialization. This does not offer any guarantee on the result however it has proven to be very effective in practice. As the Hessian is easily obtained from g_i' (21), a Newton method is used. The initial point ω_{init} is chosen as the argument of the maximum value among all the $\bar{g}_i$, $i = 1, \ldots, n$ computed at step 6 of Algorithm 1, *i.e.*

$$\omega_{init} = \arg\max\{\bar{g}_1, \bar{g}_2, \ldots, \bar{g}_n\}. \quad (25)$$

Remark 4. Standard optimization tools can be used to compute Γ. This is why the algorithm is not detailed here.

Remark 5. Note that Γ and $\bar{\Gamma}$ can also be constructed to bound the $\mathcal{H}_\infty$-norm of the system over a finite frequency-interval Ω. Indeed, it only implies to restrict the search space to this specific interval Ω. In practice, this results in evaluating the functions g_i at the bounds of the interval for $\bar{\Gamma}$ and to choose the initial point ω_{init} in Ω for Γ.

3. APPLICATION OF THE BOUNDS IN FREQUENCY-LIMITED MODEL APPROXIMATION

In this section, the bounds presented in Theorem 3 are integrated in a $\mathcal{H}_{2,\Omega}$ model approximation method. They enable to have information on the $\mathcal{H}_\infty$-norm of the error for reasonable numerical costs given the considered model approximation framework. Indeed Problem 1 is addressed by looking for the poles $\hat{\lambda}_k$, residues $\hat{\phi}_k$ and direct feedthrough $\hat{D}$ of the reduced-order model $\hat{\mathbf{H}}$ described by its transfer function $\hat{H}$,

$$\hat{H}(s) = \sum_{k=1}^{r} \frac{\hat{\phi}_k}{s - \hat{\lambda}_k} + \hat{D}. \quad (26)$$

Such a parametrization has already been considered for the optimal $\mathcal{H}_2$ model approximation problem in Beattie and Gugercin (2009) and the extension to the frequency-limited case has been proposed in Vuillemin et al. (2014). The approach consists in expressing the $\mathcal{H}_{2,\Omega}$ approximation error (4) as a function of the reduced order model poles and residues and to differentiate it to obtain the first-order optimality conditions. Again, for sake of simplicity, both models are supposed to be strictly proper, *i.e.* $D = \hat{D} = 0$ but the general case can be handled as well (see Vuillemin et al. (2014)).

3.1 $\mathcal{H}_{2,\Omega}$ approximation : first-order optimality conditions

Grounded on the poles/residues expression of the $\mathcal{H}_{2,\Omega}$-norm presented in Theorem 1, the $\mathcal{H}_{2,\Omega}$-norm of the approximation error (4) between the initial large-scale model H and the low order one $\hat{H}$ is then expressed in Theorem 4 as a function of the poles $\hat{\lambda}_i$ and residues $\hat{\phi}_i$, $i = 1, \ldots, r$, of the low-order model.

Theorem 4. Given a stable n-th order model H given as (5), a stable r-th order model $\hat{H}$ given as (26) and a

$$\frac{\partial \mathcal{J}_{\mathcal{H}_{2,\Omega}}}{\partial \hat{\lambda}_m^*} = -\sum_{i=1}^{r} \frac{\hat{c}_m^* \hat{c}_i^T \hat{b}_i \hat{b}_m^H}{(\hat{\lambda}_i + \hat{\lambda}_m^*)} \left(\frac{\hat{\mathbf{a}}_{\omega,i} + \hat{\mathbf{a}}_{\omega,m}^*}{(\hat{\lambda}_i + \hat{\lambda}_m^*)} + \frac{2\omega}{\pi(\hat{\lambda}_m^{*2} + \omega^2)} \right) + \sum_{i=1}^{n} \frac{\hat{c}_m^* c_i^T b_i \hat{b}_m^H}{(\lambda_i + \hat{\lambda}_m^*)} \left(\frac{\mathbf{a}_{\omega,i} + \hat{\mathbf{a}}_{\omega,m}^*}{(\lambda_i + \hat{\lambda}_m^*)} + \frac{2\omega}{\pi(\hat{\lambda}_m^{*2} + \omega^2)} \right) \quad (28)$$

$$\frac{\partial \mathcal{J}_{\mathcal{H}_{2,\Omega}}}{\partial \hat{b}_m^*} = \sum_{i=1}^{r} \frac{\hat{b}_i^T \hat{c}_i \hat{c}_m^H}{\hat{\lambda}_i + \hat{\lambda}_m^*} \left(\hat{\mathbf{a}}_{\omega,i} + \hat{\mathbf{a}}_{\omega,m}^* \right) - \sum_{i=1}^{n} \frac{b_i^T c_i \hat{c}_m^H}{\lambda_i + \hat{\lambda}_m^*} \left(\mathbf{a}_{\omega,i} + \hat{\mathbf{a}}_{\omega,m}^* \right) \quad (29)$$

$$\frac{\partial \mathcal{J}_{\mathcal{H}_{2,\Omega}}}{\partial \hat{c}_m^*} = \sum_{i=1}^{r} \frac{\hat{c}_i^T \hat{b}_i \hat{b}_m^H}{\hat{\lambda}_i + \hat{\lambda}_m^*} \left(\hat{\mathbf{a}}_{\omega,i} + \hat{\mathbf{a}}_{\omega,m}^* \right) - \sum_{i=1}^{n} \frac{c_i^T b_i \hat{b}_m^H}{\lambda_i + \hat{\lambda}_m^*} \left(\mathbf{a}_{\omega,i} + \hat{\mathbf{a}}_{\omega,m}^* \right) \quad (30)$$

frequency interval $\Omega = [0, \omega]$, $\omega > 0$, the $\mathcal{H}_{2,\Omega}$ error $\mathcal{J}_{\mathcal{H}_{2,\Omega}}$ (4) between H and $\hat{H}$ can be expressed as

$$\mathcal{J}_{\mathcal{H}_{2,\Omega}} = \|H\|_{\mathcal{H}_{2,\Omega}}^2 + \|\hat{H}\|_{\mathcal{H}_{2,\Omega}}^2 \cdots - \sum_{i=1}^{n} \sum_{k=1}^{r} \frac{\mathbf{tr}\left(\phi_i \hat{\phi}_k^T\right)}{\lambda_i + \hat{\lambda}_k} \left(\mathbf{a}_{\omega,i} + \hat{\mathbf{a}}_{\omega,k} \right), \quad (27)$$

where $\mathbf{a}_{\omega,i} = \frac{2}{\pi}\mathbf{atan}\left(\frac{\omega}{\lambda_i}\right)$ and $\hat{\mathbf{a}}_{\omega,k} = \frac{2}{\pi}\mathbf{atan}\left(\frac{\omega}{\hat{\lambda}_k}\right)$.

Proof : See Vuillemin et al. (2014). □

Remark 6. (Computation of the $\mathcal{H}_{2,\Omega}$-norm). Note that if the eigenvalues and eigenvectors of the initial model are available, then evaluating (27) is numerically cheap since it only involves matrix and vectors products (see Vuillemin et al. (2014) for more details).

The residues of the reduced-order model $\hat{\phi}_i$, $i = 1, \ldots, r$, are not directly used as optimization variables. Indeed, these residues must be of rank 1 for the reduced-order model $\hat{\mathbf{H}}$ given by the equation (26) to be of order r. A convenient way to handle this constraint consists in expressing the residues as outer product of two vectors $\hat{c}_i \in \mathbb{C}^{1\times n_y}$ and $\hat{b}_i \in \mathbb{C}^{1\times n_u}$, *i.e.* $\hat{\phi}_i = \hat{c}_i^T \hat{b}_i$ for $i = 1, \ldots, r$. Problem 1 is finally restricted to the determination of $\hat{c}_i$, $\hat{b}_i$ and $\hat{\lambda}_i$, $i = 1, \ldots, r$ (in the strictly proper case) which minimizes the approximation error $\mathcal{J}_{\mathcal{H}_{2,\Omega}}$. For notation consistency, the initial model's residues ϕ_i are also written as $\phi_i = c_i^T b_i$ where $c_i \in \mathbb{C}^{1\times n_y}$ and $b_i \in \mathbb{C}^{1\times n_u}$ $(i = 1, \ldots, n)$.

The approximation error $\mathcal{J}_{\mathcal{H}_{2,\Omega}}$ is a function of $r(1 + n_y + n_u)$ parameters in the strictly proper case. Since only $r\,(n_y + n_u)$ parameters are required to describe a n_y outputs, n_u inputs model of order r, the problem is slightly over-parametrized. To decrease the number of decision variables, additional constraints could be added like it has been done in the $\mathcal{H}_2$ case Beattie and Gugercin (2009). Yet here, only unconstrained optimization is considered so that the problem fit the complex optimization framework stated in Sorber et al. (2012). In this article, the authors address the optimization of non-holomorphic functions $f(z, z^*)$ by constructing optimization schemes based on the scaled conjugate cogradient $2\frac{\partial f}{\partial z^*}$. The same procedure is applied here with the approximation error $\mathcal{J}_{\mathcal{H}_{2,\Omega}}$ and its conjugate cogradient is presented in Theorem 5.

Theorem 5. Given a n-th order model $H(s)$ and a r-th order model $\hat{H}(s)$ described by (5) and (26), respectively, the complex derivatives of the approximation error $\mathcal{J}_{\mathcal{H}_{2,\Omega}}$ (27) with respect to $\hat{\lambda}_m^*$, $\hat{b}_m^*$ and $\hat{c}_m^*$ $(m = 1, \ldots, r)$ are given by equations (28), (29) and (30), respectively.

Proof : The gradient is obtained through straight derivation of the error expression (27). □

Remark 7. (Computation of the gradient). Despite its apparent complexity, the conjugate cogradient of $\mathcal{J}_{\mathcal{H}_{2,\Omega}}$ can also be computed efficiently through Hadamard, matrix and vector products.

3.2 An optimization algorithm for model approximation

Algorithm 2 Descent Algorithm for Residues and Poles Optimization (**DARPO**)

Require: $A \in \mathbb{R}^{n\times n}$, $B \in \mathbb{R}^{n\times n_u}$, $C \in \mathbb{R}^{n_y\times n}$, $\Omega = [0\ \omega]$ with $\omega > 0$ and $r \in \mathbb{N}^*$.

1: Compute the eigenvalues of A and their associated eigenvectors.
2: Choose an initial point z_0 composed of $\hat{\lambda}_i^{(0)}$, $\hat{c}_i^{(0)}$, $\hat{b}_i^{(0)}$, $i = 1, \ldots, r$.
3: k ← 0.
4: **while not converged do**
5: Compute $\mathcal{J}_{\mathcal{H}_{2,\Omega}}(z_k)$ and $\frac{\partial \mathcal{J}_{\mathcal{H}_{2,\Omega}}}{\partial z^*}|_{z=z_k}$ through the equations (27), (28), (29) and (30), respectively.
6: [Optional] : Compute the $\mathcal{H}_\infty$-bounds $\bar{\Gamma}$ (and Γ) of the error system.
7: Set $p_k = -2\frac{\partial \mathcal{J}_{\mathcal{H}_{2,\Omega}}}{\partial z^*}|_{z=z_k}$.
8: Choose α_k such that $\mathcal{J}_{\mathcal{H}_{2,\Omega}}(z_k + \alpha_k p_k)$ satisfies the complex strong Wolfe conditions.
9: Set $z_{k+1} = z_k + \alpha_k p_k$.
10: k ← k+1.
11: **end while**
12: Use $\hat{\lambda}_i^{(k)}$, $\hat{c}_i^{(k)}$, $\hat{b}_i^{(k)}$, $i = 1, \ldots, r$ to construct $\hat{\mathbf{H}} = \left(\hat{A}, \hat{B}, \hat{C}\right)$.

Both Theorem 4 and Theorem 5 are used in a gradient descent procedure called **DARPO** and presented in Algorithm 2. Note that computing the bound $\bar{\Gamma}$ at step 6 is done using Algorithm 1 but does not require to solve any eigenvalue problem. Indeed, the eigenvalues and residues of both models are known and can be used directly. Similarly, computing Γ only involve the optimization process and no additional eigenvalue problem. Note that the error can be computed at each iteration or just at the end. The impact on the computation time is illustrated in Section 4. Besides, the following remarks can be made on this algorithm :

- At step 7, the descent direction is symbolically chosen as the opposite of the conjugate gradient, but in practice, a quasi-newton procedure (BFGS) is implemented and leads to better performances.
- At step 12, the reduced-order model's realization is constructed by arbitrary choosing eigenvectors $\hat{X} =$

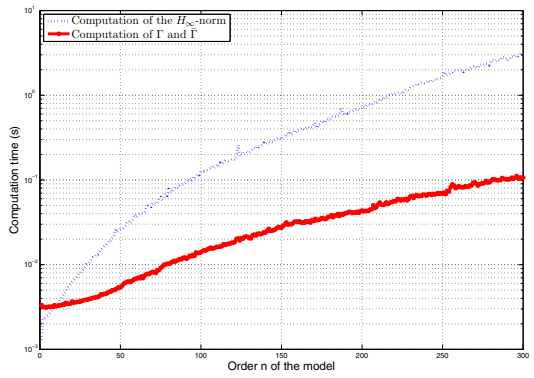

Fig. 1. Computation times of the $\mathcal{H}_\infty$-norm, Γ and $\bar{\Gamma}$ of random models with an increasing order n.

$[\hat{x}_1, \ldots, \hat{x}_r] \in \mathbb{C}^{r\times r}$ associated to the eigenvalues $\hat{\lambda}_i$, $i = 1, \ldots, r$.

- Since the eigenvalues and eigenvectors of the initial model are required, this algorithm is dedicated to medium-scale models approximation for which these quantities can be computed.

4. APPLICATION

4.1 Illustration of the bounds

The first test consists in computing the $\mathcal{H}_\infty$-norm (with Matlab's routine), Γ and $\bar{\Gamma}$ of randomly generated systems which order n varies from 1 to 300 with $n_y = n_u = 5$ in order to show the good scalability of the method. For each order n, the computation time of each routine is measured 100 times, Figure 1 compares the computations times and in Table 1 (left), the ratio of the bounds overs the true $\mathcal{H}_\infty$-norm are presented. The second test is similar but here, the order n is fixed to 10 while the number of inputs and outputs is increased from 1 to 300 [1] (with $n_y = n_u$). Again, the computation times are measured 100 times for each number of inputs/outputs. The computation times are plotted on Figure 2 together with the ratios of the bounds over the $\mathcal{H}_\infty$-norm. Those ratios are also presented in Table 1 (right).

Table 1. Ratios of the bounds over the real $\mathcal{H}_\infty$-norm for varying order n (left) and varying number of inputs/outputs (right).

varying n	Γ	$\bar{\Gamma}$	varying n_y, n_u	Γ	$\bar{\Gamma}$
min	1	1	min	1	1
mean	1.13	1.26	mean	1.26	1.43
max	1.53	2.56	max	2.33	2.42
var	0.014	0.069	var	0.07	0.11

Figure 1 shows that the bounds are seemingly faster to compute than the real $\mathcal{H}_\infty$-norm. This comes from the underlying eigenvalue problem solver which is very efficient. Yet with mean ratios value of 1.13 and 1.26 (Table 1, left), both Γ and $\bar{\Gamma}$ are relatively close to the real $\mathcal{H}_\infty$-norm. As expected, increasing the number of inputs and outputs make both bounds more conservative, as presented

[1] Given the nature of the bounds, the number of inputs and outputs is more likely to impact their quality.

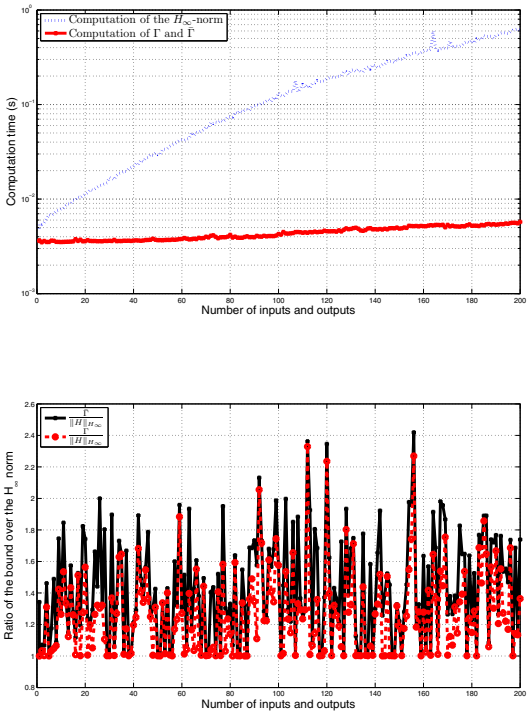

Fig. 2. Ratios and computation times of the $\mathcal{H}_\infty$-norm, Γ and $\bar{\Gamma}$ of random models with an increasing number of inputs and outputs $n_y = n_u$ going from 1 to 100.

in Table 1 (right). Indeed, the mean values of Γ and $\bar{\Gamma}$ are now 1.26 and 1.43. However, we can see on Figure 2 (bottom plot) that there is not a clear increase of the ratio as n_y and n_u grow. Besides, the number of inputs and outputs has only few impact on the computation times of the bounds compared to the impact it has on the computation of the true $\mathcal{H}_\infty$-norm.

4.2 Comparison with the balanced truncation's bound

In this example, the ISS model (270 states, 3 outputs, 3 inputs) from Leibfritz and Lipinski (2003) is reduced for several order r going from 2 to 30 with the balanced truncation (BT). For each reduced-order model, the real $\mathcal{H}_\infty$-norm of the error, the bound given by the balanced truncation and the proposed bounds Γ and $\bar{\Gamma}$ are computed. The results are plotted on Figure 3.

We can see that both Γ and $\bar{\Gamma}$ are tighter than the bound given by the balanced truncation (see for instance Antoulas (2005)) whereas they do not require more computation. Obviously though, the proposed bounds are not computable a priori and require the reduced order model to be constructed.

*4.3 Behaviour of the bound with **DARPO***

The ISS model is reduced to several orders r going from 2 to 30 with **DARPO**. For each order, the following relative quantities are computed $\frac{\|H-\hat{H}\|_{\mathcal{H}_\infty}}{\|H\|_{\mathcal{H}_\infty}}$ and $\frac{\Gamma(H-\hat{H})}{\|H\|_{\mathcal{H}_\infty}}$, $\frac{\bar{\Gamma}(H-\hat{H})}{\|H\|_{\mathcal{H}_\infty}}$ and the computation time of the reduced-order model is measured *(i)* without the computations of the bounds *(ii)* with computation of the bounds at each iteration *(iii)* with

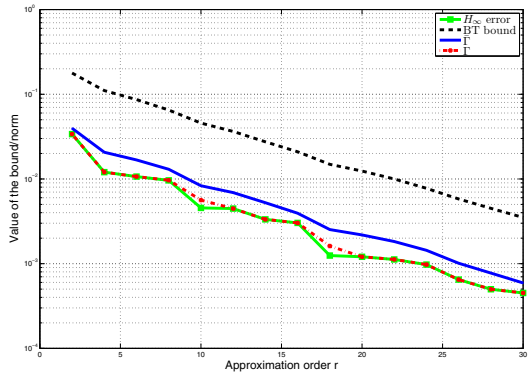

Fig. 3. Comparison of the two proposed bounds with the balanced truncation's one by approximation of the ISS model to a varying order r.

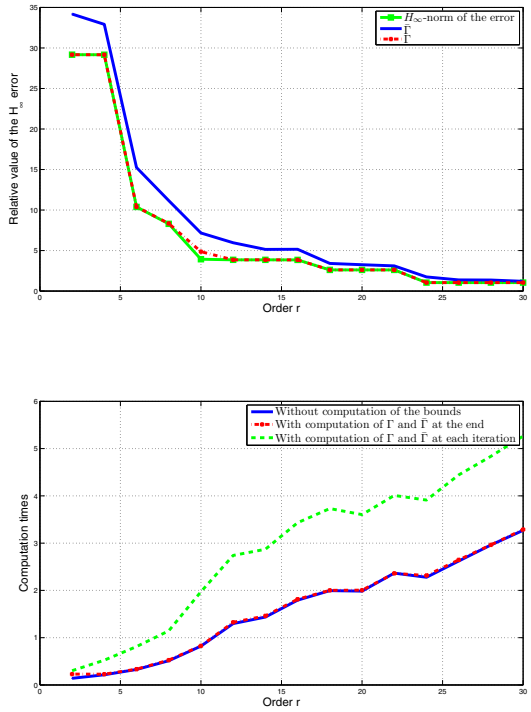

Fig. 4. Comparison of the bounds and the real $\mathcal{H}_\infty$-norm of the error when reducing the ISS model with DARPO for several orders r.

computations of the bounds at the end of the algorithm. The results are plotted on Figure 4.

We can see that both bounds are very close to the real $\mathcal{H}_\infty$-norm and does not really impact the computation time when they are only computed at the end of the algorithm (*i.e.* for the final approximation error).

5. CONCLUSION

In this paper, two upper bounds on the $\mathcal{H}_\infty$-norm of a MIMO LTI dynamical systems have been introduced. Those bounds are grounded on the relation between the $\mathcal{H}_\infty$-norm and the frequency-limited $\mathcal{H}_2$-norm. Their computation is done by exploiting the poles/residues formulation of this norm and is fast whenever the eigenvalues and eigenvectors of the system are available. The two bounds have been integrated into DARPO, a descent algorithm for optimal frequency-limited model approximation, thus giving an indication on the $\mathcal{H}_\infty$-norm of the approximation error which is interesting since only few model reduction techniques offer such information. The efficiency of the bounds, both in terms of computation times and closeness to the $\mathcal{H}_\infty$-norm, has been illustrated through several numerical examples.

REFERENCES

Anderson, M.R., Emami-Naeni, A., and Vincent, J. (1991). Measures of merit for multivariable flight control. Technical report, Systems Control Technology Inc, Palo Alto, California, USA.

Antoulas, A.C. (2005). *Approximation of Large-Scale Dynamical Systems*. Society for Industrial and Applied Mathematics.

Beattie, C. and Gugercin, S. (2009). A trust region method for optimal $\mathcal{H}_2$ model reduction. In *proceedings of the Joint 48th IEEE Conference on Decision and Control and 28th Chinese Control Conference*, 5370–5375.

Bugarin, F., Henrion, D., and Lasserre, J. (2011). Minimizing the sum of many rational functions. Available as http://arxiv.org/abs/1102.4954.

Gawronski, W. and Juang, J. (1990). Model reduction in limited time and frequency intervals. *International Journal of Systems Science*, 21(2), 349–376.

Gugercin, S., Antoulas, A.C., and Beattie, C. (2008). $\mathcal{H}_2$ model reduction for Large-Scale linear dynamical systems. *SIAM Journal on Matrix Analysis and Applications*, 30(2), 609–638.

Haber, H.E. (2011). The complex inverse trigonometric and hyperbolic functions. University of California.

Leibfritz, F. and Lipinski, W. (2003). Description of the benchmark examples in *COMPl$_e$ib* 1.0. Technical report, University of Trier.

Masi, A., Wallin, R., Garulli, A., and Hansson, A. (2010). Robust finite-frequency $\mathcal{H}_2$ analysis. In *Proceedings of the 49th IEEE Conferance on Decision and Control*, 6876 –6881.

Petersson, D. (2013). *A Nonlinear Optimization Approach to $\mathcal{H}_2$-Optimal Modeling and Control*. Ph.D. thesis, Linköping University.

Poussot-Vassal, C., Loquen, T., Vuillemin, P., Cantinaud, O., and Lacoste, J. (2013). Business jet large-scale model approximation and vibration control. In *In Proceedings of the 11th IFAC International Workshop on Adaptation Learning in COntrol and Signal Processing (ALCOSP'13)*, 199–204.

Sorber, L., Van Barel, M., and De Lathauwer, L. (2012). Unconstrained optimization of real functions in complex variables. *SIAM J. Optim*, 22, 879–898.

Van Dooren, P., Gallivan, K.A., and Absil, P.A. (2008). $\mathcal{H}_2$-optimal model reduction of MIMO systems. *Applied Mathematics Letters*, 21(12), 1267–1273.

Vuillemin, P., Poussot-Vassal, C., and Alazard, D. (2012). A spectral expression for the frequency-limited $\mathcal{H}_2$-norm. Available as http://arxiv.org/abs/1211.1858.

Vuillemin, P., Poussot-Vassal, C., and Alazard, D. (2014). Poles Residues Descent Algorithm for Optimal Frequency-Limited $\mathcal{H}_2$ Model Approximation. Accepted to the 13th European Control Conference.